

ANALYSIS OF RETINAL CAPILLARIES IN PATIENTS WITH TYPE 1 DIABETES AND NONPROLIFERATIVE DIABETIC RETINOPATHY USING ADAPTIVE OPTICS IMAGING

MARCO LOMBARDO, MD, PhD,* MARIACRISTINA PARRAVANO, MD,*
SEBASTIANO SERRAO, MD, PhD,* PIETRO DUCOLI, MD,* MARIO STIRPE, MD,*
GIUSEPPE LOMBARDO, MENG, PhD†‡

Purpose: To illustrate a noninvasive method to analyze the retinal capillary lumen caliber in patients with Type 1 diabetes.

Methods: Adaptive optics imaging of the retinal capillaries were acquired in two parafoveal regions of interest in eyes with nonproliferative diabetic retinopathy and unaffected controls. Measures of the retinal capillary lumen caliber were quantified using an algorithm written in Matlab by an independent observer in a masked manner. Comparison of the adaptive optics images with red-free and color wide fundus retinography images was also assessed.

Results: Eight eyes with nonproliferative diabetic retinopathy (eight patients, study group), no macular edema, and preserved visual acuity and eight control eyes (eight healthy volunteers; control group) were analyzed. The repeatability of capillary lumen caliber measurements was $0.22 \mu\text{m}$ (3.5%) with the 95% confidence interval between 0.12 and $0.31 \mu\text{m}$ in the study group. It was $0.30 \mu\text{m}$ (4.1%) with the 95% confidence interval between 0.16 and $0.43 \mu\text{m}$ in the control group. The average capillary lumen caliber was significantly narrower in eyes with nonproliferative diabetic retinopathy ($6.27 \pm 1.63 \mu\text{m}$) than in the control eyes ($7.31 \pm 1.59 \mu\text{m}$, $P = 0.002$).

Conclusion: The authors demonstrated a noninvasive method to analyze, with microscopic scale of resolution, the lumen of retinal capillaries. The parafoveal capillaries were narrower in patients with Type 1 diabetes and nonproliferative diabetic retinopathy than in healthy subjects, showing the potential capability of adaptive optics imaging to detect pathologic variations of the retinal microvascular structures in vaso-occlusive diseases.

RETINA 0:1–10, 2013

Diabetic retinopathy (DR) is responsible for ~12% of new cases of blindness between the ages of 45 and 74 years in the developed world.^{1,2} According to the most known pathophysiological model of DR, chronic hyperglycemia leads to blood flow abnormalities and pathologic changes of the retinal microvascular structures. The earliest alterations are represented by a thickening of the

capillary basement membrane, a loss of pericytes, an increased number of acellular capillaries, increased plasma viscosity, reduced capillary blood flow velocity, and decreased level of antithrombotic activity of the vascular endothelium.^{3–12} All these changes contribute to increased capillary permeability, through the inner blood–retinal barrier breakdown, and to capillary occlusion.^{13,14} These phenomena lead to retinal hypoxia and accordingly to retinal ischemia that are precursors of the major complications of DR, such as the development of retinal neovascularization and retinal detachment.

An increasing number of reports have been published showing that the changes of major retinal vessels' caliber can be used as markers of early

From the *Fondazione G.B. Bietti IRCCS, Rome, Italy; †CNR-IPCF Unit of Support Cosenza, University of Calabria, Rende, Italy; and ‡Vision Engineering, Rome, Italy.

None of the authors have any financial/conflicting interests to disclose.

Reprint requests: Marco Lombardo, MD, PhD, Fondazione G.B. Bietti IRCCS, Via Livenza 3, 00198 Rome, Italy; e-mail: mlombardo@visioeng.it

vascular dysfunction associated with diabetes and diabetes complications.^{11,13,15–18} The retinal arteriolar and venular diameters have been found to be larger in individuals with diabetes; nevertheless, the pattern of associations seemed to vary in the population.¹⁸ The larger venular caliber has been additionally associated with retinopathy severity.¹⁸

An important retinal microstructure for the early diagnosis of several retinal diseases, including diabetes, is the capillary network. Retinal nonperfusion first appears at the level of the capillary. Pathologic variations of capillaries in patients with diabetes are in general evidenced as an enlargement of the foveal avascular zone (FAZ) area, because of capillary loss, and a reduction of the perifoveal capillary blood flow velocity.^{12,19–21} Although fluorescein angiography (FA) currently represents the most used technique in clinical settings to resolve the microvasculature network, the retinal capillaries have also been visualized using a variety of non-invasive imaging approaches, including entoptic viewing, retinal function imager, optical microangiography, and high-resolution imaging tools, such as adaptive optics (AO) scanning laser ophthalmoscopy, flood-illuminated AO ophthalmoscopy, and AO optical coherence tomography (OCT).^{22–36} Adaptive optics technology, when implemented in an ophthalmoscope or in an OCT, has allowed noninvasive visualization and quantification of retinal capillaries in healthy eyes and eyes with retinal diseases.^{30–36}

In this paper, we illustrated a noninvasive method to analyze the retinal capillaries' lumen caliber using a flood-illumination AO retinal camera. We evaluated the repeatability of the method by measuring the parafoveal retinal capillaries in patients with Type 1 diabetes and nonproliferative diabetic retinopathy (NPDR) and in age-matched healthy subjects.

Materials and Methods

The study was approved by a local Ethical Committee and adhered to the tenets of the Declaration of Helsinki. After detailed explanation of the procedure, written informed consent was obtained from all patients. The inclusion criteria included patients with diagnosis of Type 1 diabetes mellitus >9 years earlier and mild signs of NPDR according to the Early Treatment Diabetic Retinopathy Study severity scale (defined as the presence of at least 1 microaneurysm and/or mild hemorrhages and/or hard exudates and/or cotton wool spots),^{37,38} 20/20 best-corrected visual acuity, and no previous diagnosis of macular edema. Exclusion criteria included the coexistence of any other systemic disease (e.g., hypertension) or any other ocular disease, including ocular

media opacities, and previous ocular surgery. Healthy subjects, with no history of systemic or eye diseases, were recruited as control group.

All subjects received a complete eye examination, including a non-contact ocular biometry using the IOL Master (Carl Zeiss Meditec, Inc, Jena, Germany), retinal imaging using a Heidelberg Retina SLO/SD OCT (Spectralis; Heidelberg Engineering GmbH, Heidelberg, Germany), and color fundus retinography (TRC-50 DX; Topcon Instr. Corp, Tokyo, Japan). A flood-illumination AO retinal camera prototype (rtx1; Imagine Eyes, Orsay, France) was used to evaluate the retinal capillaries. The AO retinal camera has been described more completely elsewhere.^{39,40}

Adaptive Optics Imaging

The AO imaging sessions were conducted after the pupil was dilated with 1 drop of 1% tropicamide. During AO imaging, fixation was maintained by having the patient fixate the internal target of the instrument moved by the investigator at fixed retinal locations, considering that the fixation coordinates, $x = 0^\circ$, $y = 0^\circ$, correspond to the foveal fixation reference point. A series of overlapping images of the microvasculature around the foveal fixation reference point were acquired in each eye to generate images of the capillaries surrounding the FAZ. The acquired images were combined to create an AO montage. The montage was compared with the subject's SLO fundus image and color fundus photograph previously examined by a retinal specialist (M.P.) to assess the grade of DR. The SLO and color fundus photographs showing the major retinal vessels were used for comparison with AO images to identify the locations of arterioles and venules in regions of interest (ROI; Figure 1). The retinal capillaries were evaluated in 2 ROI centered at 1) $x = 1.5^\circ$ temporal/ $y = 1.8^\circ$ superior eccentricity and at 2) $x = 1.0^\circ$ nasal/ $y = 1.8^\circ$ inferior eccentricity. The ROI were selected to represent the zones at which the average density and lumen diameter of the parafoveal retinal capillaries were previously shown to be greater than other zones closer to the border of the FAZ.^{31,32,41}

A sequence of 40 frames, illuminating a 4° field size, was acquired in 1 eye of each subject (binary randomization). The deformable mirror of the *rtx1* was used to select the appropriate plane of focus. The focal plane was adjusted to acquire images of the capillaries of the inner nuclear layer to maximize the sharpness of vascular images. Each imaging session consisted of focusing through the retina at 10 μm steps from the photoreceptor layer to the nerve fiber layer using the *rtx1* software interface. In correspondence of both ROI, the capillary network of the inner

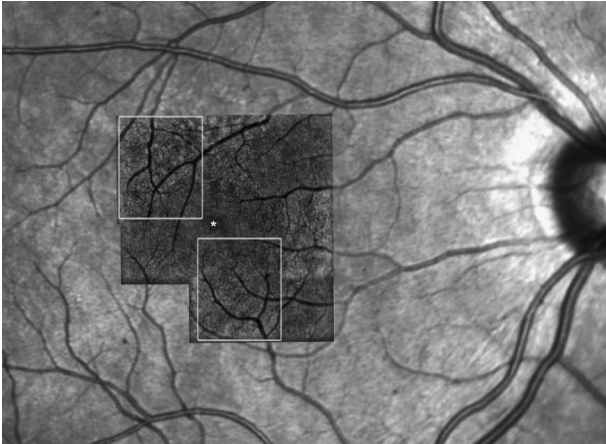


Fig. 1. A series of AO overlapping images were acquired in each eye and used to create a montage to compare the retinal microstructures with those taken by wide-field fundus photographs. The retinal capillaries were investigated in 2 ROI centered at 1.8° superior to 1.5° temporal and 1.8° inferior to 1.0° nasal (gray squares) from the foveal fixation reference point (asterisk).

nuclear layer was imaged 210 μm to 230 μm anteriorly to the photoreceptor layer.

After the acquisition, frames exhibiting large motion artifacts because of eye movement or blinking were manually removed before processing (in general, three to five frames per sequence). Then, a proprietary program, provided by the manufacturer, has been used to correct for distortions within frames of the raw image sequence and to correlate and average the frames to produce a final image with enhanced signal-to-noise ratio compared with the single exposure frame.⁴⁰ The final image was saved as an 8-bit gray-level intensity image. No further post-processing methods were applied to the image. Each final image was converted to micrometers using model

eye parameterized by the biometry measurements from each eye obtained with the IOL Master, according to the nonlinear formula of Drasdo and Fowler and using the Gullstrand eye as a model.^{40,42–44}

Capillary Identification

To unambiguously define the retinal capillaries, topologic description of vascular trees by the Horton–Strahler and generation nomenclatures (i.e., large arteriole, small arteriole, and capillary) was performed, as previously described.⁴⁵ Vessel orders were defined according to the convergence of smaller branches. Levels of branching were defined as generations in the vascular tree. The order was increased if 2 segments of equal order join at a bifurcation, as shown in Figure 2.

Capillary Lumen Measurement

The contrast of the retinal vessel's image depends on the interaction of light and the blood vessel. The light that comes back to the imaging camera is a combination of the light scattered from the vessel wall, the back scattered light from the blood flowing inside the vessel lumen, and the back scattered light from other retinal structures, including photoreceptors and nerve fiber bundles. Using an AO flood-illumination retinal camera, the lumen of a blood vessel appears as a streak of variable diameter and morphology, depending on the vessel order; however, it always shows the same pattern, consisting of a central high-intensity channel and two peripheral darker channels (probably because of the curved vessel wall). This pattern was observed both in single frame and average frames result, thus

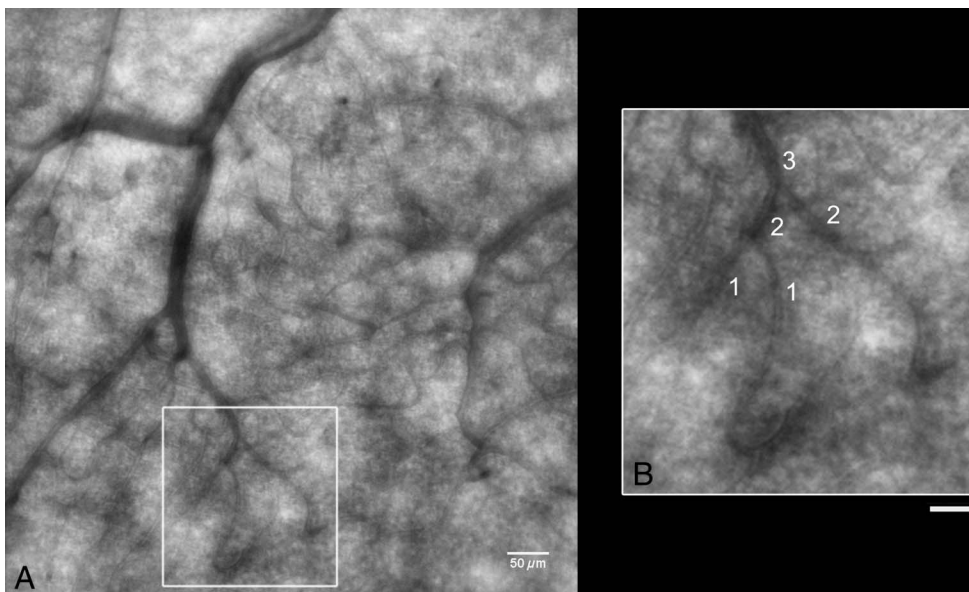


Fig. 2. A. Adaptive optics image showing the capillary network of a superotemporal parafoveal ROI (scale bar, 50 μm). B. High-magnification area from panel A (white square; scale bar, 25 μm) showing details of the microvascular tree. The Horton–Strahler topologic description of vascular trees starts at the capillary level and proceeds centripetally. The order is increased if two segments of equal order join at a bifurcation: two capillaries (1) join together to form a first-order arteriole (2) and two first-order arterioles join together to form a second-order arteriole (3).

excluding the possibility that it could be because of the averaging of the frames to reduce noise.

Various methods have been developed to estimate the retinal blood vessel diameter from the intensity pattern. In general, the blood vessel intensity profile was fitted with a Gaussian function, and the vessel width was estimated as the width between two preset thresholds on the Gaussian curve.^{36,46,47} When computed in this manner, the vessel lumen diameter can be greatly underestimated in an en face ophthalmoscopy image because the vessel width does not account for the dark regions in the peripheral lumen, assuming that these represent the vessel wall.^{48,49}

In this work, the cross-section lumen caliber, D_s , was extracted using a semiautomated procedure, including manual selection of the capillaries in each ROI and automated quantification via an algorithm written in Matlab (software version 7.0; The MathWorks, Inc., Natick, MA). For each extracted intensity profiles, the algorithm defined as D_s the distance between the two intensity minima peaks, that correspond to the lumen periphery (i.e., the two peripheral dark channels), interposed between the maximum intensity peak corresponding to the lumen center. To minimize errors because of oblique extraction of intensity profile and/or no perpendicular incident light camera illumination, the measurements were confined only to those capillaries in which the difference between the intensity levels of the 2 darkest peaks was less than a threshold (<10 gray value; i.e., <5% of the intensity level of the image). An independent observer (G.L.), who was masked to the eye's group, selected the capillaries in

each ROI. No preference was given other than that the capillary had to be visually distinguishable from the background reflectance and clearly focused. For each ROI, three to seven capillaries were analyzed, and for each identified capillary, three adjacent cross-sectional profiles were selected. The measurements were automatically stored in a text array and used for statistics, as shown in Figure 3.

Repeatability and Measurement Error

The repeatability of capillary measurements was calculated based on the within-subject standard deviation (σ_w), that is, the common standard deviation of repeated measurements. To get the common within-subject standard deviation, we averaged the variances, that is, the squares of the standard deviations, of the repeated measures for each subject. The within-subject standard deviation was chosen as an index of measurement error, as discussed by Bland and Altman.^{50,51} The repeatability was defined as $2.77\sigma_w$ and reported both in terms of the measurement unit (micrometers) as well as a percentage of the mean. The 95% confidence interval for repeatability was calculated as $2.77\sigma_w/\sqrt{2n(m-1)}$, where n is the number of subjects and m is the number of observations for each subject.

Statistical Analysis

Statistical analysis was performed using the SPSS software (version 17.0; SPSS, Inc., Chicago, IL). Data were expressed as mean \pm standard deviation. The analysis of variance was performed for the statistical

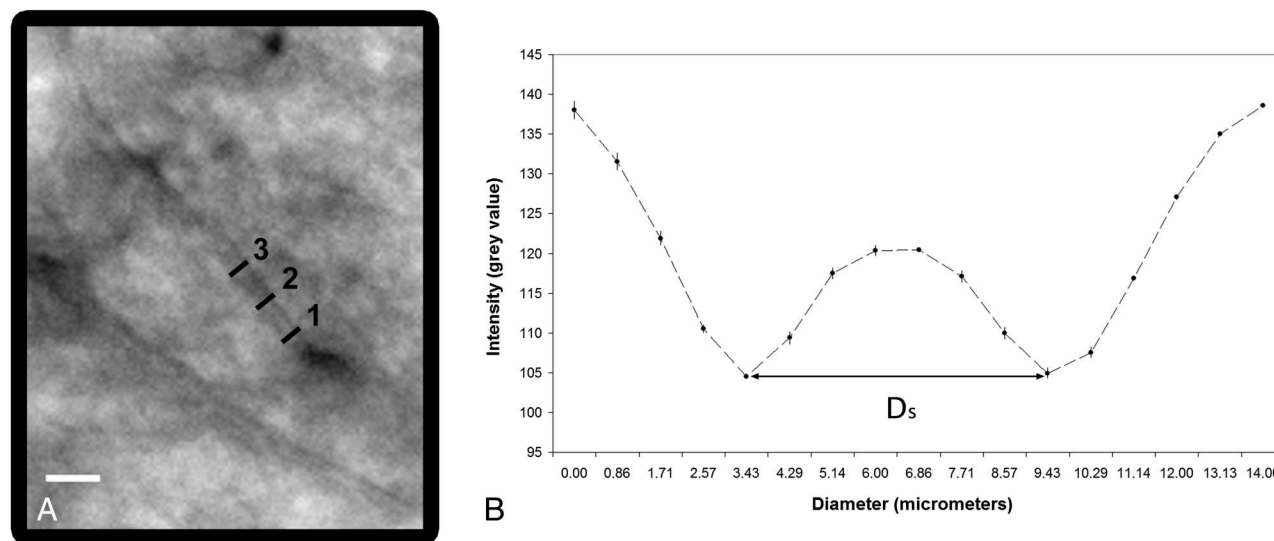


Fig. 3. Average lumen caliber of a retinal capillary as measured in this study. **A.** The AO retinal image shows location of three capillary points (black lines) that were selected for lumen diameter measurements. Scale bar, 20 μm . **B.** The three measurements were registered, averaged, and plotted as shown. Error bars in the plot represent ± 1 SD. The semiautomated method of capillary caliber measurements showed a high repeatability. D_s represents the average cross-section capillary diameter.

analysis of the capillary lumen caliber. The achieved power of the statistical analysis (β) into detecting significance of the differences in the values between NPDR and control eyes was calculated. Statistical significance was set at $P < 0.05$.

Results

Eight patients with NPDR (4 men and 4 women; Table 1) were included in the study group and 8 subjects (3 men and 5 women) in the control group. The mean age of the study group was 39.50 ± 5.96 years (range, 33–52 years old), and the mean duration of diabetes was 14.88 ± 4.05 years (range, 10–21 years). The mean A1c form of glycohemoglobin (HbA1c) level was $7.50 \pm 0.73\%$. All patients had 20/20 or better best-corrected visual acuity and did not complain any vision loss or metamorphopsia since the onset of diabetes. They had no history or signs of previous macular edema, lens opacification, or previous ocular surgery. No difference in age was measured in comparison with the control group (38.29 ± 8.44 years; range, 27–50 years old; one-way analysis of variance, $P > 0.05$). The average axial length of the tested eye was 23.99 ± 1.27 mm and 24.02 ± 1.06 mm in the study and control groups, respectively. The average spherical equivalent refraction was -1.38 ± 1.77 diopter and -1.36 ± 1.06 diopter, respectively.

The average linear distance of the superotemporal ROI's center from the foveal fixation was 671 and 646 μm in NPDR and control eyes, respectively; the average distance of the inferonasal ROI's center from the foveal fixation was 589 and 568 μm , respectively. The within-subject standard deviation (σ_w) was 0.08 and 0.11 μm in the study and control groups, respectively. The repeatability of capillary lumen caliber measurements was 0.22 μm (3.5%) with the 95% confidence interval between 0.12 and 0.31 μm in the study group.

Table 1. Characteristics of the Patients with Type 1 Diabetes and NPDR

Patient	Age (Years)	Gender	Duration of Diabetes (Years)	HbAc1 Level (%)	BCVA (logMAR)
AFL01	36	F	17	6	0.0
BCI02	38	F	21	7.2	0.0
CNT03	36	M	11	8	-0.2
DMS04	33	M	16	8.2	0.0
ETF05	44	M	11	7.2	-0.1
FMR06	52	M	10	8	-0.1
GRM07	38	F	19	7.4	-0.1
HVP08	39	F	14	8	0.0

BCVA, best-corrected visual acuity; F, female; M, male.

It was 0.30 μm (4.1%) with the 95% confidence interval between 0.16 and 0.43 μm in the control group.

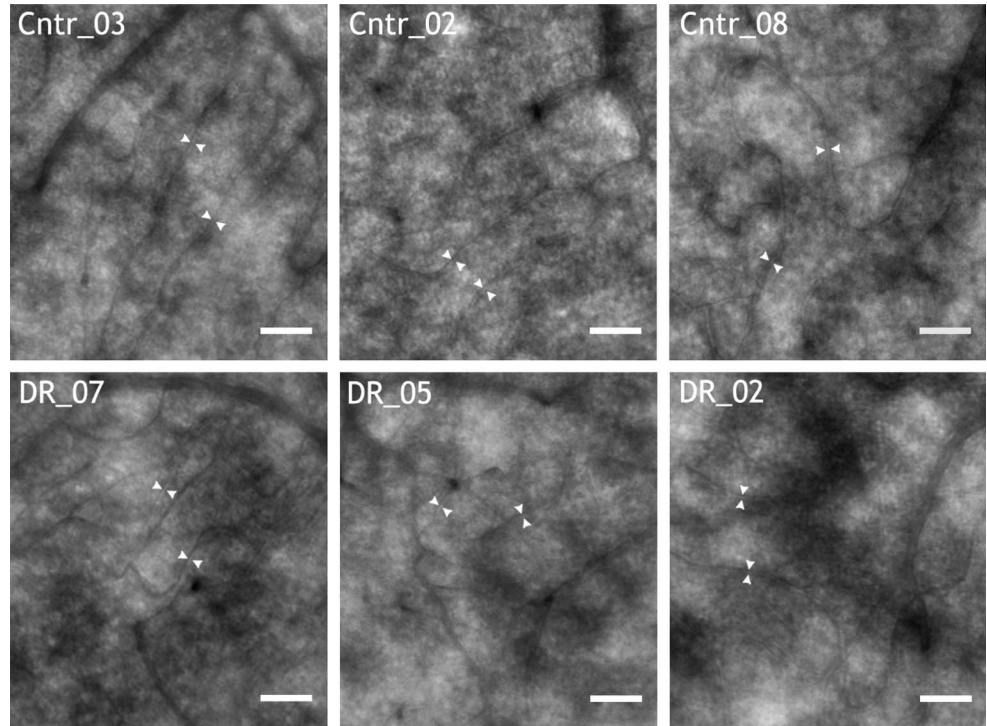
The retinal capillaries appeared as faint vessel segments intersecting each other and forming a network among arterioles and venules both in NPDR and in control eyes. Capillaries were not resolved by SLO or color fundus retinography in any eye. The average lumen of retinal capillaries was significantly narrower in NPDR eyes ($6.27 \pm 1.63 \mu\text{m}$) than in controls ($7.31 \pm 1.59 \mu\text{m}$, $P = 0.002$, $\beta = 86\%$). On average, the retinal capillary lumen was 15% narrower in NPDR eyes than in control eyes (Figure 4).

Black dots were seen along the capillaries' course in both NPDR and control eyes. The range of width of these objects was between 5.80 and 19.30 μm ; no further analysis was done to discriminate whether these features may represent perforant branching elements and/or focal capillary dilations (i.e., saccular microaneurysms) because it was beyond the aim of the present work. Occasionally, in NPDR eyes, in correspondence of the venous end of retinal capillaries, there were also objects that might be presumptive fusiform microaneurysms (Figure 5); such objects were not detected in AO images of control eyes neither were identified in SLO or color fundus photographs. Other features, corresponding to microhemorrhages, were seen in NPDR eyes. The hemorrhages appeared as dark spots of different shape and dimension that were clearly focused at the inner retina. In correspondence of the hemorrhage itself, a dark spot with defocused margins was projected on the photoreceptor layer precluding the ability to resolve the cone photoreceptors (masking effect). All the identified hemorrhages were greater than 20 μm and were also resolved by SLO and color fundus retinography (Figure 5).

Discussion

It is well known that the changes of the retinal vasculature caliber, shape, and permeability carry important information regarding the state of the microcirculation in the eye.^{6,9,10,14,16–18,52,53} Noninvasive detection of pathologic vasculature changes in DR is typically performed by dilated fundus examination, color fundus photography, and SLO. Abnormalities of the smaller vessels and capillaries are currently evaluated in clinical settings via FA.^{41,54} In mild NPDR, FA can reveal microaneurysms and nonperfusion areas as, for example, enlarged FAZ and enlarged perifoveal intercapillary areas.^{20,21} These microvascular abnormalities have been shown to be clinically significantly correlated with the progression of retinopathy and visual loss.^{13,18,21,55} Fluorescein angiography, however, requires intravenous injection of a fluorescent dye agent that can lead to

Fig. 4. High-magnification AO images of the microvasculature network in a ROI of three controls (upper row) and three NPDR cases (lower row). The average lumen diameter of the capillaries shown (arrowheads) is $7.08 \pm 1.22 \mu\text{m}$ in controls and $6.31 \pm 1.42 \mu\text{m}$ in NPDR eyes, respectively. Scale bars are $50 \mu\text{m}$.

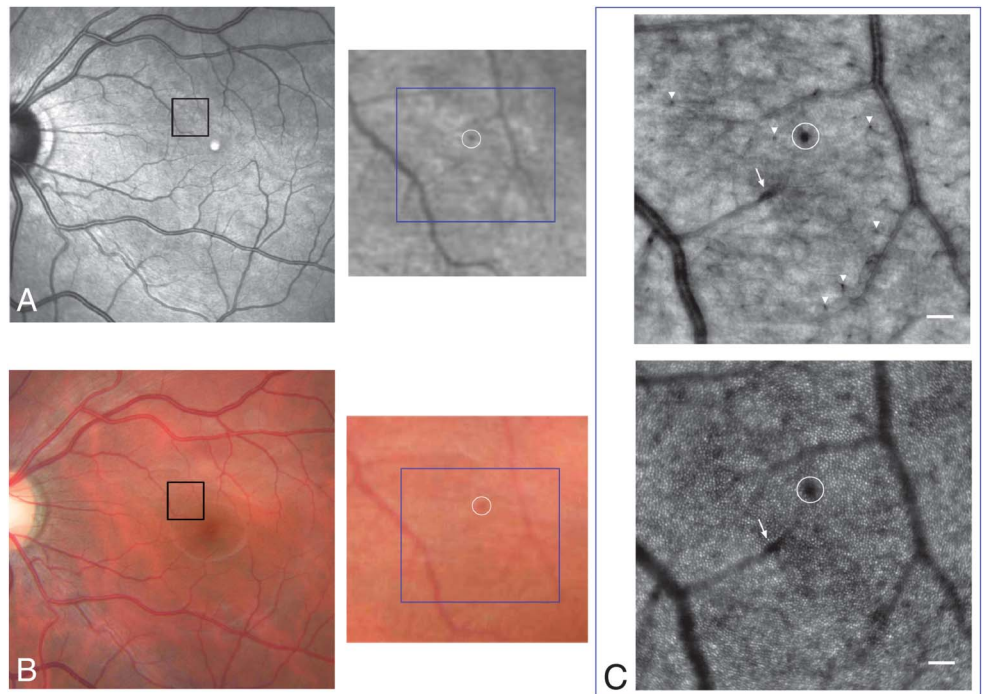


unintended systemic complications. Given the potential for rare major side effects, routine use of FA in evaluating DR is not usually performed, principally reserving this investigation for the assessment and management of

diabetic macular edema and retinal periphery. Moreover, FA is inappropriate to screen DR.

Adaptive optics retinal imaging provides the researcher with a noninvasive tool capable to obtain

Fig. 5. A. Wide-field SLO image in a 33-year-old male patient with Type 1 diabetes and NPDR. The high-magnification image of a parafoveal region (black square) shows a microhemorrhage (white circle). **B.** Color fundus photograph of the same eye and high-magnification view of the same region. **C.** Adaptive optics images of the same region showing the vessel layer (upper) and the photoreceptor layer (lower), respectively. An improved resolution of the small retinal vessels and capillary network can be achieved via AO imaging in comparison with wide-field fundus imaging. The retinal capillaries form a network between larger arterioles and venules. The frequent punctate objects seen along the course of capillaries (arrowheads) may correspond to vertical or steeply oblique capillary branches that dive to vessels located in shallow and/or deep inner layers, as seen in laboratory studies^{10,41,52} or using an AO OCT.³⁶ They may also be focal dilation of the capillary wall. The dot hemorrhage (white circle; diameters, $15 \times 32 \mu\text{m}$) can be easily distinguished from other features by identifying its shape and margins both at the nerve-vessel and photoreceptor retinal layers. The arrow highlights a presumptive fusiform microaneurysm ($22 \times 38 \mu\text{m}$) located at the venous end of a retinal capillary.



high-resolution images of the microvasculature. In this study, we evaluated the repeatability of a method to analyze the lumen caliber of retinal capillaries in patients with diabetes. Using an AO flood-illumination retinal camera, the lumen of a blood vessel shows a typical pattern, consisting of a central high-intensity channel and two peripheral darker channels. The reason for the difference in intensity between the central and peripheral vessel lumen could be because of 1) biologic factors, including the curved vessel wall, the different shear rate of erythrocytes near the wall with those flowing in the central lumen, the contribution of highly scattering regions around the vessel (e.g., photoreceptors and nerve fiber bundles)^{11,12,20,34,35,56} and 2) technical reasons, as described in the Materials and Methods section.^{49,57,58} Considering that we image an en face representation of a cylindrical vessel from the top, the central bright stripe could also depend on scattering and specular reflections of light from the vessel wall.

The capability to resolve retinal capillaries and small vessels has been shown for all existing AO ophthalmic imaging modalities.^{30–36,49,57–62} Furthermore, a variety of image processing approaches have been used to provide excellent visualization of the macular capillary network.^{30–34,62} Tam et al³³ evaluated the parafoveal capillary network in patients with Type 2 diabetes. They showed a capillary dropout and a higher tortuosity of the arteriovenous channels in patients with no retinopathy than in healthy controls. An enlargement of the FAZ was found in 1 eye of a patient with Type 1 diabetes and severe NPDR over a period of 16 months.³⁴ The combined longitudinal assessment of the FAZ area and the capillary lumen caliber by AO imaging might bring valuable information on DR progression in patients. Adaptive optics images of retinal microvasculature were also used to characterize the blood flow.^{49,61} Zhong et al⁴⁹ measured the blood velocity of erythrocytes in healthy subjects: by focusing on a blood vessel, they directly visualized erythrocytes as moving bright dots smaller than the larger, intermittent intensity variations arising from leukocytes. A significant reduction in the capillary blood velocity in patients with diabetes and no retinopathy has been shown in previous work.^{13,20,56} The detection of preclinical abnormalities of retinal microcirculation may potentially represent an additional advantage of AO retinal imaging in patients with diabetes.

In this study, images of the retinal capillaries were taken at two distances from the foveal fixation (i.e., the superotemporal and inferior-nasal ROI), taking into consideration that 1) the early pathologic changes of the capillary network were found at the posterior pole

temporally to the optic disk,^{5,6} 2) the rim of the FAZ was shown to extend to a maximum of 600 μm from the foveal center,^{20,31,32,36,61} and 3) the capillary density was shown to increase with eccentricity from the border of the FAZ to $\sim 1,000$ μm eccentricity, though with individual differences.⁴¹

Across the parafoveal ROI, the retinal capillaries formed a polygonal mesh of intersecting elements between arterioles and venules. This pattern was seen both in NPDR and control eyes. Near the FAZ, the retinal capillaries were previously shown to create a three-dimensional mesh of two or more planes through the inner retina.^{41,63–66} In this study, punctuate objects were observed along the course of capillaries, likely corresponding to vertical or steeply oblique capillary branches that dived to vessels located in shallow and/or deep inner layers^{30,41,45} or to focal bulge of the capillary wall (e.g., saccular microaneurysm).⁵ In correspondence of the venous end of capillaries, we found objects that could be presumptive fusiform microaneurysms.^{5,67} Microaneurysms are microvascular abnormalities consequent to endothelial cell and blood rheologic dysfunctions and are often observed in NPDR eyes with FA.^{5–13} The microaneurysm width was previously found to range between 15 and 70 μm , depending on the duration of diabetes, the DR severity, and the region of the retina where they were measured.^{5,6} We did not analyze these objects because it was beyond the scope of the present work.

The capillary lumen caliber was shown to be significantly narrower in NPDR eyes than age-matched controls. The average capillary lumen of eyes with NPDR was 15% narrower than healthy eyes of age-matched subjects. The results cannot be explained by the narrower lumen in diabetic eyes arising from imaging artifacts or biases: the repeatability of measurements was high ($\leq 4.1\%$) both in NPDR and in control eyes, further showing a low measurement error (≤ 0.11 μm).

In laboratory studies, the average capillary lumen caliber ranged between 6 and 7 μm across a retinal area located between 300 and 1,200 μm eccentricity from the fovea,^{41,45} favorably comparing to the values found in our population. In a pivotal study, Rha et al⁵⁷ aimed to characterize the capability of an AO flood-illumination camera to image the human retina. They showed that the capillary diameter ranged between 5 and 7 μm at 1.25° eccentricity in a healthy adult. The axial profile of human retinal capillaries proximal to the FAZ has been shown to range between an average 5.1 ± 1.4 μm using AO OCT³⁶ and 4.7 ± 0.8 μm using FA.⁴¹ It is, however, well known that the capillaries proximal to the FAZ rim are smaller than capillaries at greater eccentricities.^{36,41,66} The capillary size varies

considerably even in the same subject. A high degree of geometric and topological heterogeneity has been found in the macular vasculature of primates and humans.^{41,45} The capillary network is constituted of vessels of increasingly larger size at greater eccentricity from the foveal center. At the FAZ rim, there is only a single capillary bed located in the inner nuclear layer, whereas at increasing distances from the FAZ rim, the retinal microvasculature is multilaminar with the capillary beds forming a web of 10 μm to 15 μm thickness in the inner nuclear layer.⁶¹ We avoided to include in our analysis capillaries with oblique orientation, confining our measurements to those parts of the capillaries in which we were able to confirm the orientation as perpendicular to the incident AO retinal camera beam.³⁴ Similar approaches were used to measure the lumen of peripapillary capillaries of the nerve fiber layer using a fluorescence adaptive optics SLO⁶⁸ or the lumen of capillaries near the FAZ using ultrahigh-resolution AO OCT.³⁶ We did not attempt to measure the retinal capillaries lumen variation with eccentricity because it was beyond the scope of this work. Further investigation to understand and quantify the heterogeneities in the macular capillary network in patients is expected.^{41,45,61,69}

Pathologic changes of the retinal vessels are found in the majority of patients having Type 1 diabetes for 10 years or longer. The fundamental abnormalities of DR are an increased retinal vascular permeability and a progressive retinal capillary closure.^{5,6,11–13,70,71} The pathogenesis of these vascular changes is not yet entirely known: vascular degeneration is thought to start with a hyperglycemia-induced insult that drives subsequent microvascular changes. The thickening of the capillary basement membrane, by accumulation of advanced glycosylation end products as a function of plasma glucose concentration, is one of the most established pathologic pathway of vascular damage in diabetes. Further mechanisms involve the compromise of the antithrombotic and antifibrinolytic activity of the vascular endothelium^{11,12} and an increased leukocyte–endothelial cell adhesion and entrapment (retinal leukostasis) in retinal capillaries, as a consequence of localized low-grade inflammatory process.^{70–72} All these factors may affect vascular integrity and functionality by altering the inner blood–retinal barrier and progressively obstructing the capillary lumen.⁸

Adaptive optics imaging may give insights into how DR affects the retinal capillaries in vivo. Repeatable measurements of capillary lumen caliber were obtained in this study; nevertheless, standardization of the technique is needed to ensure a determination about whether the capillary lumen changes over time in a longitudinal study.

Key words: adaptive optics, diabetic retinopathy, retinal capillary.

Acknowledgments

The authors are thankful to David Merino, PhD (ICFO, Castelldefels, Spain), for his valuable comments and revision of the manuscript.

References

1. Klein R, Knudtson MD, Lee KE, et al. The Wisconsin Epidemiologic Study of Diabetic Retinopathy XXIII: the twenty-five-year incidence of macular edema in persons with type 1 diabetes. *Ophthalmology* 2009;116:497–503.
2. Fong DS, Aiello L, Gardner TW, et al. Diabetic retinopathy. *Diabetes Care* 2003;26:S99–S102.
3. Cunha-Vaz JG. Pathophysiology of diabetic retinopathy. *Br J Ophthalmol* 1978;62:351–355.
4. Moore J, Bagley S, Ireland G, et al. Three dimensional analysis of microaneurysms in the human diabetic retina. *J Anatomy* 1999;194:89–110.
5. Kern TS, Engerman RL. Vascular lesions in diabetes are distributed non-uniformly within the retina. *Exp Eye Res* 1995;60:545–549.
6. Yu DY, Cringle SJ, Su EN, et al. Pathogenesis and intervention strategies in diabetic retinopathy. *Clin Exp Ophthalmol* 2001;29:164–166.
7. Engerman RL. Pathogenesis of diabetic retinopathy. *Diabetes* 1989;38:1203–1206.
8. Durham JT, Herman IM. Microvascular modifications in diabetic retinopathy. *Curr Diab Rep* 2011;11:253–264.
9. Sander B, Larsen M, Engler C, et al. Early changes in diabetic retinopathy: capillary loss and blood-retina barrier permeability in relation to metabolic control. *Acta Ophthalmol* 1994;72:553–559.
10. Hammes HP, Martin S, Federlin K, et al. Aminoguanidine treatment inhibits the development of experimental diabetic retinopathy. *Proc Natl Acad Sci USA* 1991;88:11555–11558.
11. Fekete GT, Buzney SM, Ogasawara H, et al. Retinal circulatory abnormalities in type 1 diabetes. *Invest Ophthalmol Vis Sci* 1994;35:2968–2975.
12. Konno S, Fekete GT, Yoshida A, et al. Retinal blood flow changes in type 1 diabetes. A long-term follow up study. *Invest Ophthalmol Vis Sci* 1996;37:1140–1148.
13. Barchetta I, Riccieri V, Vasile M, et al. High prevalence of capillary abnormalities in patients with diabetes and association with retinopathy. *Diabet Med* 2011;28:1039–1044.
14. Do Carmo A, Ramos P, Reis A, et al. Breakdown of the inner and outer blood retinal barrier in Streptozotocin-Induced diabetes. *Exp Eye Res* 1998;67:569–575.
15. Liew G, Sharrett AR, Kronmal R, et al. Measurement of retinal vascular caliber: issues and alternatives to using the arteriole to venule ratio. *Invest Ophthalmol Vis Sci* 2007;48:52–57.
16. Klein R, Myers CE, Lee KE, et al. Changes in retinal vessel diameter and incidence and progression of diabetic retinopathy. *Arch Ophthalmol* 2012;130:749–755.
17. Nguyen TT, Wang JJ, Wong TY. Retinal vascular changes in pre-diabetes and prehypertension: new findings and their research and clinical implications. *Diabetes Care* 2007;30:2708–2715.

18. Klein R, Klein BEK, Moss SE, et al. The relation of retinal vessel caliber to the incidence and progression of diabetic retinopathy. XIX: The Wisconsin Epidemiologic Study of Diabetic Retinopathy. *Arch Ophthalmol* 2004;122:76–83.
19. Nguyen TT, Wang JJ, Sharrett AR, et al. Relationship of retinal vascular caliber with diabetes and retinopathy. *Diabetes Care* 2008;31:544–549.
20. Arend O, Wolf S, Jung F, et al. Retinal microcirculation in patients with diabetes mellitus: dynamic and morphological analysis of perifoveal capillary network. *Br J Ophthalmol* 1991;75:514–518.
21. Sakata K, Funatsu H, Harino S, et al. Relationship between macular microcirculation and progression of diabetic macular oedema. *Ophthalmology* 2006;113:1385–1391.
22. Bradley A, Zhang H, Applegate RA, et al. Entoptic image quality of the retinal vasculature. *Vision Res* 1998;38:2685–2696.
23. Applegate RA, Bradley A, van Heuven WA, et al. Entoptic evaluation of diabetic retinopathy. *Invest Ophthalmol Vis Sci* 1997;38:783–791.
24. Izhaky D, Nelson DA, Burgansky-Eliash Z, Grinvald A. Functional imaging using the retinal function imager: direct imaging of blood velocity, achieving fluorescein angiography-like images without any contrast agent, qualitative oximetry, and functional metabolic signals. *Jpn J Ophthalmol* 2009;53:345–351.
25. Dubis AM, Hansen BR, Cooper RF, et al. Relationship between the foveal avascular zone and foveal pit morphology. *Invest Ophthalmol Vis Sci* 2012;53:1628–1636.
26. An L, Wang RK. In vivo volumetric imaging of vascular perfusion within human retina and choroids with optical microangiography. *Opt Express* 2008;16:11438–11452.
27. Kim DY, Fingler J, Werner JS, et al. In vivo volumetric imaging of human retinal circulation with phase-variance optical coherence tomography. *Biomed Opt Express* 2011;2:1504–1513.
28. Makita S, Jaillon F, Yamanari M, et al. Comprehensive in vivo micro-vascular imaging of the human eye by dual-beam-scan Doppler optical coherence angiography. *Opt Express* 2011;19:1271–1283.
29. Zotter S, Pircher M, Torzicky T, et al. Visualization of microvasculature by dual-beam phase-resolved Doppler optical coherence tomography. *Opt Express* 2011;17:19:1217–1227.
30. Schmoll T, Singh ASG, Blatter C, et al. Imaging of the parafoveal capillary network and its integrity analysis using fractal dimension. *Biomed Opt Express* 2011;2:1159–1168.
31. Popovic Z, Knutsson P, Thaug J, et al. Noninvasive imaging of human foveal capillary network using dual-conjugate adaptive optics. *Invest Ophthalmol Vis Sci* 2011;52:2649–2655.
32. Tam J, Martin JA, Roorda A. Noninvasive visualization and analysis of parafoveal capillaries in humans. *Invest Ophthalmol Vis Sci* 2010;51:1691–1698.
33. Tam J, Dhamdhere KP, Tiruveedhula P, et al. Disruption of the retinal parafoveal capillary network in type 2 diabetes before the onset of diabetic retinopathy. *Invest Ophthalmol Vis Sci* 2012;52:9257–9266.
34. Tam J, Dhamdhere KP, Tiruveedhula P, et al. Subclinical capillary changes in non-proliferative diabetic retinopathy. *Optom Vis Sci* 2012;89:E692–E703.
35. Uji A, Hangai M, Ooto S, et al. The source of moving particles in parafoveal capillaries detected by adaptive optics scanning laser ophthalmoscopy. *Invest Ophthalmol Vis Sci* 2012;53:171–178.
36. Wang Q, Kocaoglu OP, Cense B, et al. Imaging retinal capillaries using ultrahigh-resolution optical coherence tomography and adaptive optics. *Invest Ophthalmol Vis Sci* 2011;52:6292–6299.
37. Early Treatment Diabetic Retinopathy Study Research Group. Grading diabetic retinopathy from stereoscopic color fundus photographs: an extension of the modified Airlie House classification. ETDRS report number 10. *Ophthalmology* 1991;98:823–833.
38. Early Treatment Diabetic Retinopathy Study Research Group. Photocoagulation for diabetic macular edema: Early Treatment Diabetic Retinopathy Study report number 1. *Arch Ophthalmol* 1985;103:1796–1806.
39. Lombardo M, Lombardo G, Ducoli P, Serrao S. Adaptive optics photoreceptor imaging. *Ophthalmology* 2012;119:1498–1498e2.
40. Lombardo M, Serrao S, Ducoli P, Lombardo G. Variations in the image optical quality of the eye and the sampling limit of resolution of the cone mosaic with axial length in young adults. *J Cataract Refract Surg* 2012;38:1147–1155.
41. Weinhaus RS, Burke JM, Delori FC, et al. Comparison of fluorescein angiography with microvascular anatomy of macaque retinas. *Exp Eye Res* 1995;61:1–16.
42. Drasdo N, Fowler CW. Non-linear projection of the retinal image in a wide-angle schematic eye. *Br J Ophthalmol* 1974;58:709–714.
43. Coletta NJ, Watson T. Effect of myopia on visual acuity measured with laser interference fringes. *Vis Res* 2006;46:636–651.
44. Li KY, Tiruveedhula P, Roorda A. Intersubject variability of foveal cone photoreceptor density in relation to eye length. *Invest Ophthalmol Vis Sci* 2010;51:6858–6867.
45. Yu PK, Balaratnasingam C, Cringle SJ, et al. Microstructure and network organization of the microvasculature in the human macula. *Invest Ophthalmol Vis Sci* 2010;51:6735–6743.
46. Hammer DX, Iftimia NV, Ferguson RD, et al. Foveal fine structure in retinopathy of prematurity: An Adaptive Optics Fourier Domain Optical Coherence Tomography study. *Invest Ophthalmol Vis Sci* 2008;49:2061–2070.
47. Chapman N, Witt N, Gao X, et al. Computer algorithm for the automated measurement of retinal arteriolar diameters. *Br J Ophthalmol* 2001;85:74–79.
48. Brinckmann-Hansen O, Engvold O. Microphotometry of the blood column and the light streak on retinal vessels in fundus photography. *Acta Ophthalmol* 1986;64:9–19.
49. Zhong Z, Petrig BL, Qi X, Burns S. In vivo measurement of erythrocyte velocity and retinal blood flow using adaptive optics scanning laser ophthalmoscopy. *Opt Express* 2008;16:12746–12755.
50. Bland JM, Altman DG. Measurement error proportional to the mean. *BMJ* 1996;313:106.
51. Bland JM, Altman DG. Measurement error and correlation coefficients. *BMJ* 1996;313:41.
52. Sasongko MB, Wang JJ, Donaghue KC, et al. Alterations in retinal microvascular geometry in young type 1 diabetes. *Diabetes Care* 2010;6:1331–1336.
53. Wong TY. Retinal vessel diameter as a clinical predictor of diabetic retinopathy progression: time to take out the measuring tape. *Arch Ophthalmol* 2011;129:95–96.
54. Mendis KR, Balaratnasingam C, Yu P, et al. Correlation of histological and clinical images to determine the diagnostic value of fluorescein angiography for studying retinal capillary detail. *Invest Ophthalmol Vis Sci* 2010;51:5864–5869.
55. Murakami T, Nishijima K, Sakamoto A, et al. Foveal cystoid spaces are associated with enlarged foveal avascular zone and

- microaneurysms in diabetic macular edema. *Ophthalmology* 2011;118:359–367.
56. Zhang L, Krzentowski G, Albert A, et al. Risk of developing retinopathy in diabetes control and complications trial type 1 diabetic patients with good or poor metabolic control. *Diabetes Care* 2001;24:1275–1279.
 57. Rha J, Jonnal RS, Thorn KE, et al. Adaptive optics flood-illumination camera for high-speed retinal imaging. *Opt Express* 2006;14:4552–4569.
 58. Miller DT, Kocaoglu OP, Wang Q, Lee S. Adaptive optics and the eye (super resolution OCT). *Eye (Lond)* 2011;25:321–330.
 59. Tam J, Roorda A. Speed quantification and tracking of moving objects in adaptive optics scanning laser ophthalmoscopy. *J Biomed Opt* 2011;16:036002.
 60. Li H, Lu J, Shi G, Zhang Y. Measurement of oxygen saturation in small retinal vessels with adaptive optics confocal scanning laser ophthalmoscope. *J Biomed Opt* 2011;16:110504.
 61. Tam J, Tiruveedhula P, Roorda A. Characterization of single-flow through human retinal parafoveal capillaries using an adaptive optics scanning laser ophthalmoscope. *Biomed Opt Express* 2011;2:781–793.
 62. Chui TPY, VanNasdale DA, Burns SA. The use of forward scatter to improve retinal vascular imaging with an adaptive optics scanning laser ophthalmoscope. *Biomed Opt Express* 2012;3:2537–2549.
 63. Paques M, Todayoni R, Sercombe R, et al. Structural and hemodynamic analysis of the mouse retinal microcirculation. *Invest Ophthalmol Vis Sci* 2003;44:4960–4967.
 64. Gariano RF, Iruela-Arispe ML, Hendrickson AE. Vascular development in primate retina: comparison of laminar plexus formation in monkey and human. *Invest Ophthalmol Vis Sci* 1994;35:3442–3455.
 65. Bek T, Jensen PK. Three-dimensional structure of human retinal vessels studied by vascular casting. *Acta Ophthalmol* 1993;71:506–513.
 66. Snodderly DM, Weinhaus RS, Choi JC. Neural-vascular relationships in central retina of macaque monkeys (*Macaca fascicularis*). *J Neurosci* 1992;12:1169–1193.
 67. Fleming AD, Philip S, Goatman KA, et al. Automated microaneurysm detection using local contrast normalization and local vessel detection. *IEEE Trans Med Imaging* 2006;25:1223–1232.
 68. Scoles D, Gray DC, Hunter JJ, et al. *In-vivo* imaging of retinal nerve fiber layer vasculature: imaging histology comparison. *BMC Ophthalmol* 2009;9:9.
 69. Kong X, Wang K, Sun X, Witt RE. Comparative study of the retinal vessel anatomy of rhesus monkeys and humans. *Clin Exp Ophthalmol* 2010;38:629–634.
 70. Chibber R, Ben-Mahmud BM, Chibber S, Kohner EM. Leukocytes in diabetic retinopathy. *Curr Diabetes Rev* 2007;3:3–14.
 71. Kern TS. Contributions of inflammatory processes to the development of the early stages of diabetic retinopathy. *Exp Diabetes Res* 2007;2007:95103.
 72. Luty GA, Cao J, McLeod DS. Relationship of polymorphonuclear leukocytes to capillary dropout in the human diabetic choroid. *Am J Pathol* 1997;151:707–714.